Translational Oncology
www.transonc.com

Volume 8 Number 2 April 2015 pp. 112–118 112

Therapeutic Efficacy Assessment of CK6, a Monoclonal KIT Antibody, in a Panel of Gastrointestinal Stromal Tumor Xenograft Models[1,2]

Thomas Van Looy*,[3], Agnieszka Wozniak*,[3], Giuseppe Floris†, Haifu Li*, Jasmien Wellens*, Ulla Vanleeuw*, Raf Sciot†, Maria Debiec-Rychter‡ and Patrick Schöffski*

*Laboratory of Experimental Oncology, Department of Oncology, KU Leuven and Department of General Medical Oncology, University Hospitals Leuven, Leuven Cancer Institute, Leuven, Belgium; †Department of Pathology, KU Leuven and University Hospitals Leuven, Leuven, Belgium; ‡Department of Human Genetics, KU Leuven and University Hospitals Leuven, Leuven, Belgium

Abstract

We evaluated the efficacy of CK6, a KIT monoclonal antibody, in a panel of human gastrointestinal stromal tumor (GIST) xenograft models. Nude mice were bilaterally transplanted with human GIST xenografts (four patient derived and two cell line derived), treated for 3 weeks, and grouped as follows: control (untreated); CK6 (40 mg/kg, 3 × weekly); imatinib (50 mg/kg, twice daily); sunitinib (40 mg/kg, once daily); imatinib + CK6; sunitinib + CK6 (same doses and schedules as in the single-agent treatments). Tumor volume assessment, Western blot analysis, and histopathology were used for evaluation of efficacy. Statistical analysis was performed using Mann-Whitney U (MWU) and Wilcoxon matched-pairs tests. CK6 as a single agent only reduced tumor growth rate in the UZLX-GIST3 model ($P = .053$, MWU compared to control), while in none of the other GIST models an effect on tumor growth rate was observed. CK6 did not result in significant anti-proliferative or pro-apoptotic effects in any of the GIST models, and moreover, CK6 did not induce a remarkable inhibition of KIT activation. Furthermore, no synergistic effect of combining CK6 with tyrosine kinase inhibitors (TKIs) was observed. Conversely, in certain GIST xenografts, anti-tumor effects seemed to be inferior under combination treatment compared to single-agent TKI treatment. In the GIST xenografts tested, the anti-tumor efficacy of CK6 was limited. No synergy was observed on combination of CK6 with TKIs in these GIST models. Our findings highlight the importance of using relevant *in vivo* human tumor xenograft models in the preclinical assessment of drug combination strategies.

Translational Oncology (2015) 8, 112–118

Introduction

Gastrointestinal stromal tumors (GISTs) are the most common mesenchymal tumors of the digestive system [1]. About 95% of GISTs show expression of KIT protein by immunohistochemistry (IHC) [2]. KIT is a member of the family of class III receptor tyrosine kinases (RTKs) and is composed of an extracellular (EC) domain, consisting of five Ig-like repeats, a juxtamembrane, and a cytoplasmic kinase domain, containing an ATP-binding (TK1) and phospho-transferase (TK2) domain split by a kinase insert. In approximately 85% of clinical GIST cases, somatic activating *KIT* mutations are found, being the main molecular driver in the oncogenesis of the disease [3,4]. These mutations induce constitutional activation of KIT and its signaling mediators, resulting in a modulation of cell proliferation and survival. Another subset of GIST patients harbors

Address all correspondence to: Patrick Schöffski, MD, MPH, Department of General Medical Oncology, University Hospitals Leuven, Herestraat 49, 3000 Leuven, Belgium. E-mail: thomas.vanlooy@med.kuleuven.be

[1] Prior presentation: "Efficacy Assessment of CK6, a Monoclonal KIT Antibody, in a Panel of Gastrointestinal Stromal Tumor (GIST) Xenograft Models", poster presentation at the Connective Tissue Oncology Society Annual Meeting 2014.

[2] Research funding and CK6 were provided by ImClone Systems, a wholly owned subsidiary of Eli Lilly and Company (New York, NY). Conflict of interest: The authors declare no conflicts of interest.

[3] These authors contributed equally to this work.

Received 22 September 2014; Revised 19 February 2015; Accepted 27 February 2015

1936-523/15
http://dx.doi.org/10.1016/j.tranon.2015.02.004

Table 1. Description of Xenograft Models Used in the Study

Xenograft Model	Origin	*KIT* Mutational Status	Expected *In Vivo* Imatinib Sensitivity [16,18,30]
UZLX-GIST1	Patient biopsy	Exon 11: p.V560D, htz	Yes
UZLX-GIST2	Patient biopsy	Exon 9: p.A502_Y503dup, htz	Dose-dependent
UZLX-GIST3	Patient biopsy	Exon 11: p.W557_V559delinsF, htz	Yes
UZLX-GIST4	Patient biopsy	Exon 11: p.K558_G565delinsR, htz	Yes
GIST48	Cell line	Exon 11: pV560D, hom + exon 17: pD820A, htz	Resistant
GIST882	Cell line	Exon 13: p.K642E, hom	Yes

htz, heterozygous; hom, homozygous.

primary activating mutations in the gene encoding for platelet-derived growth factor receptor α (PDGFRA), belonging to the same RTK family as KIT [5]. The dependence of tumor cells on KIT/PDGFRA activation profiles GIST as a target for selective tyrosine kinase inhibitors (TKIs) such as imatinib. Response to imatinib has been shown to strongly depend on the *KIT/PDGFRA* genotype [6,7]. However, some patients are intolerant to imatinib, and even more importantly, the majority of treated patients will experience imatinib resistance during the course of therapy [8,9]. After imatinib failure, alternative TKIs can be considered for treatment of advanced GIST, such as sunitinib and regorafenib. Nevertheless, these TKIs provide only limited clinical benefit and time to progression seems to shorten with every consecutive line of treatment [10,11]. TKI resistance is mainly acquired through secondary missense *KIT/PDGFRA* mutations that hamper the activity of the TKIs or less frequently through genomic *KIT* amplification. Importantly, multiple synchronous resistant mutations can be present in the same patient at different metastatic sites and even within one metastatic lesion [9]. The heterogeneous nature of TKI resistance in GIST emphasizes the need to develop and test novel treatment approaches that could potentially override or delay TKI resistance.

In the majority of cases, imatinib-resistant mutations modify either the TK1 or the TK2 domain of the RTK. Mutations in TK1 can still be responsive to alternative KIT inhibitors (e.g., sunitinib), whereas those in the latter are believed to yield uniform resistance to currently available compounds [12]. However, in TKI-resistant GISTs, tumor cells still primarily rely on KIT activation as an oncogenic driver. Importantly, the ligand-binding domain remains unaffected in these TKI-resistant GISTs. Therefore, drugs targeting the EC region (ligand binding) of the KIT receptor could represent an attractive therapeutic strategy to overcome TKI resistance in GISTs. Recently, Edris et al. demonstrated that SR1, an anti-KIT monoclonal antibody, is able to inhibit growth of human GIST cell lines *in vitro* [13]. Furthermore, SR1 inhibited tumor growth also *in vivo* in GIST882 and GIST430 xenograft models. Another KIT antibody, CK6, has recently demonstrated KIT antagonist activity and tumor growth neutralizing properties in melanoma and small cell lung carcinoma [14]. In the present study, we tested the efficacy of CK6 in six GIST human xenograft models characterized by different sensitivity to standard TKI treatment.

Materials and Methods

GIST Xenografts

For this study, GIST xenografts were established by bilaterally subcutaneous transplantation of human GIST tumor fragments in female adult athymic *nu/nu* NMRI mice (Janvier Laboratories, Saint-Berthevin Cedex, France) as described before [15–18]. UZLX-GIST1, UZLX-GIST2, UZLX-GIST3, and UZLX-GIST4 models were established using biopsies or resection specimen obtained from GIST patients, treated in the Department of General Medical Oncology, University Hospitals Leuven. The GIST48 and GIST882 models were derived from tumors resulting from subcutaneous injection of cells (both cell lines were a kind gift from Dr J. A. Fletcher, Boston). A detailed characterization of the used GIST xenograft models can be found in Table 1. Collection of GIST tissue for xenografting is approved by the Medical Ethics Committee, University Hospitals Leuven. All animal experiments were conducted in accordance with Belgian law and approved by the Ethics Committee for Laboratory Animals, KU Leuven.

Drugs and Reagents

CK6 was provided by ImClone Systems (New York City, NY) in phosphate-buffered saline. Imatinib mesylate and sunitinib malate were purchased from Sequoia Research Products Ltd (Pangbourne, United Kingdom) and were dissolved, respectively, in sterile water and citric buffer (pH 3.5).

The following polyclonal or monoclonal antibodies were used for Western blot analysis and IHC: pKITY719 (recognizing human pKITY721 site), α-tubulin, and HRP-labeled anti-rabbit Signal Stain Boost IHC detection reagent were from Cell Signaling Technologies (Danvers, MA); pKITY703 was from Life Technologies; KIT (CD117), anti-rabbit Envision + System and 3′-diaminobenzidine tetrahydrochloride were from DAKO (Carpinteria, CA); β-actin and tubulin were from Sigma-Aldrich (Saint Louis, MO); Ki67 was from Thermo Scientific (Waltham, MA); cleaved PARP (Cl-PARP) was from Abcam (Cambridge, United Kingdom), and Reveal Decloaker was from Biocare Medical (Concord, CA). Western Lightning Plus-ECL enhanced chemiluminescence substrate reagents came from PerkinElmer (Waltham, MA).

Study Design

A total of 171 mice (333 tumors) was engrafted bilaterally with UZLX-GIST1 (n = 24), UZLX-GIST2 (n = 36), UZLX-GIST3 (n = 30), UZLX-GIST4 (n = 29), GIST48 (n = 29), or GIST882 (n = 23) tumors. Animals were assigned to six different groups and dosed for 3 weeks as follows: control group (untreated), CK6 group [40 mg/kg, 3× weekly; intraperitoneal (i.p.) administration], imatinib group (50 mg/kg, twice daily; orally by gavage), imatinib + CK6 group (dosed and scheduled as above), sunitinib group (40 mg/kg, once daily; orally by gavage), and sunitinib + CK6 group (dosed and scheduled as above). Tumor volume and mouse body weight were measured three times weekly and normalized for baseline values. After 3 weeks of treatment, mice were sacrificed, and tumor tissue was fixed in 4% formaldehyde or snap frozen in liquid nitrogen for histopathologic and molecular characterization.

Histologic Assessment

Tumor fragments fixed in formaldehyde were embedded in paraffin blocks and 4-μm sections were cut for hematoxylin and

eosin (H&E) and IHC. Histologic response (HR) was graded by assessing the magnitude of necrosis, myxoid degeneration, or fibrosis using the following grading scheme: 1—minimal (0-10%), 2—low (>10% and ≤50%), 3—moderate (>50% and ≤90%), and 4—high (>90%) grade [19,20]. In addition, we have also added to the grading system the area with myxoid degeneration, which is characterized by the replacement of viable tumor tissue by an amorphous matrix with low cellularity as a pattern of response to TKI treatment observed [21]. Mitotic figures and apoptotic cells were counted in 10 high power fields (0.45-mm field diameter) at ×400 magnification on H&E staining. Cl-PARP, a marker for apoptotic activity, was assessed by counting positive cells in 10 high power fields. Additionally, the antibody Ki67 was used as a measure for proliferative activity and was scored as the average of Ki67-positive tumor cells on five digital microscopic pictures taken at ×400 magnification. Microscopy was performed using the Olympus CH-300 microscope; pictures were taken with digital camera Color View (all Olympus, Tokyo, Japan).

Western Blot Analysis

Snap frozen tumors collected at the end of the experiment were used for lysate preparation for Western blot analysis, as previously described [16]. Three different tumor lysates were run for each treatment group, which were run in the adjacent lanes as group-by-group comparison. For gels comparing the effect of CK6 with imatinib or with sunitinib, we used the same lysates for control (untreated) and CK6-treated tumors. Chemiluminescence levels were registered with the FUJI-LAS Mini 3000 System (Fujifilm, Tokyo, Japan).

Statistical Analysis

Wilcoxon matched-pairs test was used for comparison of tumor volumes between day 0 and the end of the *in vivo* experiment. Mann-Whitney U (MWU) test was performed to compare between different treatment groups. A P value of $<.05$ was considered as statistically significant. For the statistical analysis, STATISTICA 12.0 (StatSoft, Tulsa, Oklahoma) software was used.

Results

Tumor Volume Assessment

Overall, irrespective of *KIT* mutational status, untreated GIST xenografts showed a 2.1-fold increase in tumor volume after 3 weeks of observation (Table 2).

In general, regardless of *KIT* genotype, imatinib reduced the tumor volume to 69% of standardized baseline values. As expected from our experience with these models and their molecular profile, a significant tumor regression was observed in the *KIT* exon 11 mutants UZLX-GIST1, UZLX-GIST3, and UZLX-GIST4. Notably, imatinib also decreased tumor volume in GIST48 as was described by our group before [18]. Furthermore, imatinib stabilized tumor volume in the GIST882 model and an increase of tumor volume was observed in UZLX-GIST2 under treatment. When all xenograft models were considered, sunitinib treatment caused the most remarkable effect on tumor volume, causing a reduction in tumor volume to 36% compared to baseline (Table 2).

CK6 treatment yielded a reduction in tumor growth rate in the UZLX-GIST3 model ($P = .053$, MWU test), whereas tumor burden increased in a rate similar to untreated control tumors in the other GIST xenograft models. We did not observe enhanced efficacy on combining CK6 with TKIs in any GIST xenograft model tested. Moreover, imatinib single-agent treatment yielded a more pronounced tumor volume reduction than imatinib + CK6 in UZLX-GIST1, UZLX-GIST2, and GIST48 xenografts but not in the GIST882 model. In addition, sunitinib was significantly more potent than sunitinib + CK6 in reducing tumor volume in the GIST48 and GIST882 models ($P < .05$, MWU test, sunitinib compared to sunitinib + CK6).

During *in vivo* experiments, mouse body weight and health status were continuously monitored. No major side effects were observed in any of the treatment arms, and the experimental treatments were well tolerated.

Histopathology

Histologic response. We assessed HR by scoring the extent of necrosis, myxoid degeneration, or fibrosis in H&E staining of the tumor specimens collected after 3 weeks of treatment (Figure 1) [19,20]. Importantly, in the GIST882 and GIST48 models, the interpretation of HR was indecisive due to the observation of necrotic and myxoid changes of the stroma in more than 50% of untreated tumors. In the UZLX-GIST2 and UZLX-GIST4 models, we observed only minimal to low HR in the majority of tumors.

In the remaining models (UZLX-GIST1 and UZLX-GIST3), HR to imatinib and even more pronounced with sunitinib was characterized by the induction of myxoid degeneration. Under imatinib, 50% of UZLX-GIST1 tumors showed grade 3 HR and the remaining tumors showed even grade 4 HR, while in ULZX-GIST3 all tumors showed grade 2 HR. Under sunitinib tumors in the UZLX-GIST1 and UZLX-GIST3 models, all showed at least grade 3 HR.

Overall, CK6 treatment yielded only minimal to low HR (grade 1 or 2) in GIST models, mainly characterized by necrosis, in ~85% of tumors, which was comparable to untreated control tumors. No enhanced histologic change in GIST tumor samples was observed on combining standard TKIs with CK6.

Table 2. Relative Tumor Volume Assessment in GIST Models after 3 Weeks of Treatment

	Relative Tumor Volume after 3 Weeks [Mean % (95% CI)]						
	All Models	*KIT*$^{exon\ 11}$			*KIT*$^{exon\ 9}$	*KIT*$^{exon\ 13}$	*KIT*$^{exon\ 11\ +\ 17}$
		UZLX-GIST1	UZLX-GIST3	UZLX-GIST4	UZLX-GIST2	GIST882	GIST48
Control	209 (81-117)	151 (106-196)	282 (172-392)	262 (206-217)	244 (198-291)	169 (132-207)	138 (99-177)
CK6	198 (81-116)	152 (111-193)	152 (63-240)	290 (210-370)	250 (211-289)	179 (143-215)	155 (118-191)
Imatinib	69 (53-79)**	21 (12-30)**	25 (18-32)**	45 (28-62)**	168 (148-188)**	100 (66-133)**	16 (11-21)**
Imatinib + CK6	84 (56-83)**	41 (23-59)**	33 (28-39)**	50 (32-67)**	194 (177-211)*	92 (75-109)**	46 (28-63)**
Sunitinib	36 (23-34)**	22 (8-35)**	23 (18-27)**	19 (10-28)**	80 (69-91)**	37 (29-46)**	15 (8-22)**
Sunitinib + CK6	43 (22-32)**	27 (1-53)**	25 (17-32)**	24 (14-34)**	62 (50-74)**	65 (46-85)**	53 (38-68)**

MWU test was performed for statistical assessment; *$P < .05$, **$P < .005$ (compared to control); CI, confidence interval.

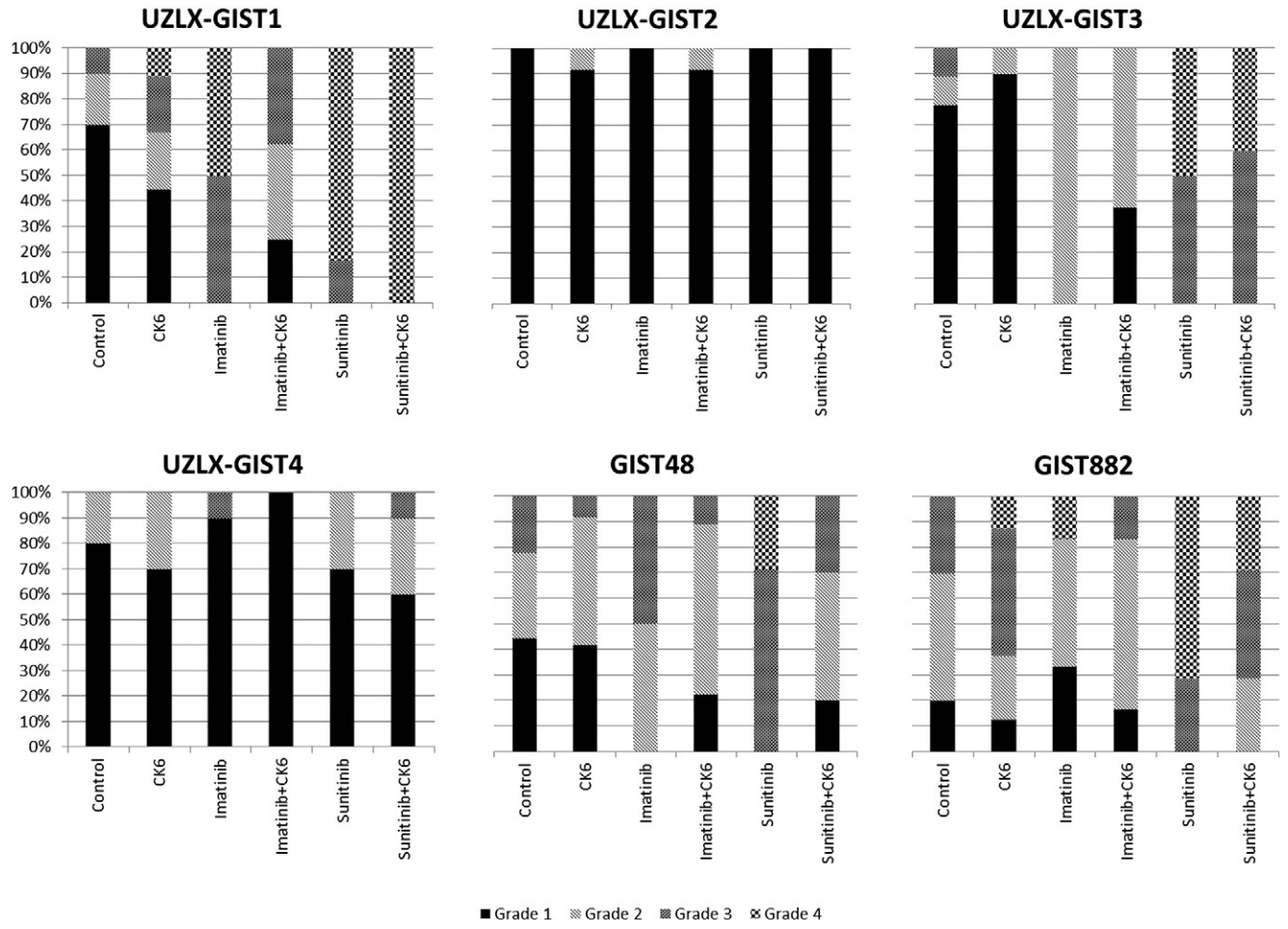

Figure 1. HR was assessed in all tested xenograft models and grouped by treatment. HR was graded by assessing the magnitude of necrosis, myxoid degeneration, and/or fibrosis on H&E staining: grade 1 (0-10%), grade 2 (>10% and ≤50%), grade 3 (>50% and ≤90%), and grade 4 (>90%).

Table 3. Histologic Assessment of Mitotic and Apoptotic Activity, Assessed on Tumors Collected after 3 Weeks of Treatment

		Xenograft Model					
		KIT$^{exon\ 11}$			*KIT*$^{exon\ 9}$	*KIT*$^{exon\ 13}$	*KIT*$^{exon\ 11\ +\ 17}$
		UZLX-GIST1	UZLX-GIST3	UZLX-GIST4	UZLX-GIST2	GIST882	GIST48
Mitosis	CK6	↑1.1	↑1.2	↑1.1	=1.0	↑1.1	=1.0
	Imatinib	↓↓↓**	↓↓↓**	↓↓↓**	↓1.5**	↓1.7	↓19.4**
	Imatinib + CK6	↓↓↓**	↓24.9**	↓↓↓**	↑1.1	↓1.8	↓6.4**
	Sunitinib	↓↓↓**	↓↓↓**	↓↓↓**	↓↓↓**	↓↓↓**	↓50.9**
	Sunitinib + CK6	↓↓↓**	↓↓↓**	↓↓↓**	↓↓↓**	↓7.8**	↓1.7**
Ki67	CK6	↑1.2	↑1.2	↑1.4**	=1.0	↑1.2	↓1.2
	Imatinib	↓50.1**	↓↓↓**	↓↓↓**	↓1.8**	↓2.1*	↓21.0**
	Imatinib + CK6	↓↓↓**	↓34**	↓↓↓**	↓1.1	↓2.4*	↓3.6**
	Sunitinib	↓↓↓**	↓↓↓**	↓↓↓**	↓39.6**	↓38.7**	↓9.4**
	Sunitinib + CK6	↓↓↓**	↓↓↓**	↓↓↓**	↓33**	↓4.1**	↓1.4*
Apoptosis	CK6	↑1.5	↓1.4	↑1.4	↑1.1	↑1.1	↑1.4
	Imatinib	↑2.4	↑4.6**	↑2.3**	↓1.5**	↓2.1**	↑2.2**
	Imatinib + CK6	↓7.5**	↑1.2	↑1.9**	↓1.1	↓3.5**	↑1.4**
	Sunitinib	↑2.3	↑8**	↑7.7**	↓5.2**	↑1.4*	↑1.7
	Sunitinib + CK6	↓17.4**	↑7.5**	↑4.4**	↓6.3**	↑1.1	↑2.1**
Cl-PARP	CK6	↑1.4	↓1.3	↑1.4	↑1.1	↓1.2	↑1.1
	Imatinib	↑1.4	↑7.2**	↑1.3	↓1.8**	↓2.1**	↑1.8**
	Imatinib + CK6	↓8.1**	=1.0	↑1.1	↓1.2*	↓4.6**	↑1.5*
	Sunitinib	↑1.8	↑11.9**	↑6.9**	↓7.4**	↓1.1	↑1.4
	Sunitinib + CK6	↓9.5**	↑10.8**	↑3.9**	↓8.3**	↓1.6	↑1.3*

MWU test was performed for statistical assessment; *$P < .05$, **$P < .005$ (compared to control).
↓↓↓—more than 100-fold decrease; H&E—H&E staining, Cl-PARP—Cl-PARP immunostaining. Results are presented as fold changes in comparison with control; upward arrows indicate increase, and downward arrows represent decrease.

Mitotic and apoptotic activity. Subsequently, we assessed the mitotic and apoptotic activity on H&E staining in the GIST xenografts after 3 weeks of treatment (Table 3).

Imatinib treatment variably reduced the mitotic activity in all xenograft models, being particularly remarkable in UZLX-GIST1, UZLX-GIST3, UZLX-GIST4 (*KIT* exon 11 mutation), and GIST48 (KIT exon 11 and exon 17 mutation) (all $P < .005$, MWU test). In the UZLX-GIST2 (*KIT* exon 9 mutation) and GIST882 (*KIT* exon 13 mutation) models, mitotic activity was reduced to a lesser extent (Table 3). Sunitinib profoundly affected mitotic activity in all GIST xenograft models ($P < .005$ in all models, MWU test).

Compared to control, mitotic activity was not significantly reduced by CK6 single treatment in any GIST xenograft model. The combination of imatinib or sunitinib with CK6 did not reduce further the mitotic activity of single TKI therapy, even resulting in a less potent effect compared to single TKI in certain xenograft models [e.g.,UZLX-GIST2, UZLX-GIST3, GIST48 for imatinib + CK6 (all $P < .05$, MWU test, imatinib *vs* imatinib + CK6) and GIST48 and GIST882 for sunitinib + CK6 ($P \leq .05$, MWU test, sunitinib *vs* sunitinib + CK6)].

Under imatinib, the apoptotic activity was significantly increased compared to control in UZLX-GIST3, UZLX-GIST4, and GIST48 ($P < .005$, MWU test). Furthermore, sunitinib significantly induced apoptosis in UZLX-GIST3, UZLX-GIST4, and GIST882 ($P < .05$, MWU test).

Single agent CK6 did not induce a significant increase in apoptotic activity in the GIST xenograft models tested. Combination of CK6 and TKI did not lead to a synergistic pro-apoptotic effect over either TKI treatment. Of note, in UZLX-GIST2 none of the treatments was able to induce a significant pro-apoptotic effect and a similar absence of pro-apoptotic activity was observed under imatinib and imatinib + CK6 in GIST882 xenografts.

In general, observations on H&E were confirmed by Ki67 and Cl-PARP immunostaining, which were used as confirmatory markers of proliferative and apoptotic activity (Table 3).

KIT Expression and Activation

Western blot analysis was performed to assess KIT expression and activation (Figure 2). As expected, imatinib induced a remarkable inhibition of KIT phosphorylation in UZLX-GIST1, UZLX-GIST3, and UZLX-GIST4 xenograft models (*KIT* exon 11 mutations). In the GIST882 and UZLX-GIST2 models (*KIT* exon 13 and exon 9 mutations, respectively), no relevant decrease in KIT phosphorylation was observed under imatinib. In the GIST48 model, in spite of the presence of a secondary *KIT* exon 17 mutation, both sunitinib and imatinib resulted in a decrease in KIT activation. Sunitinib also

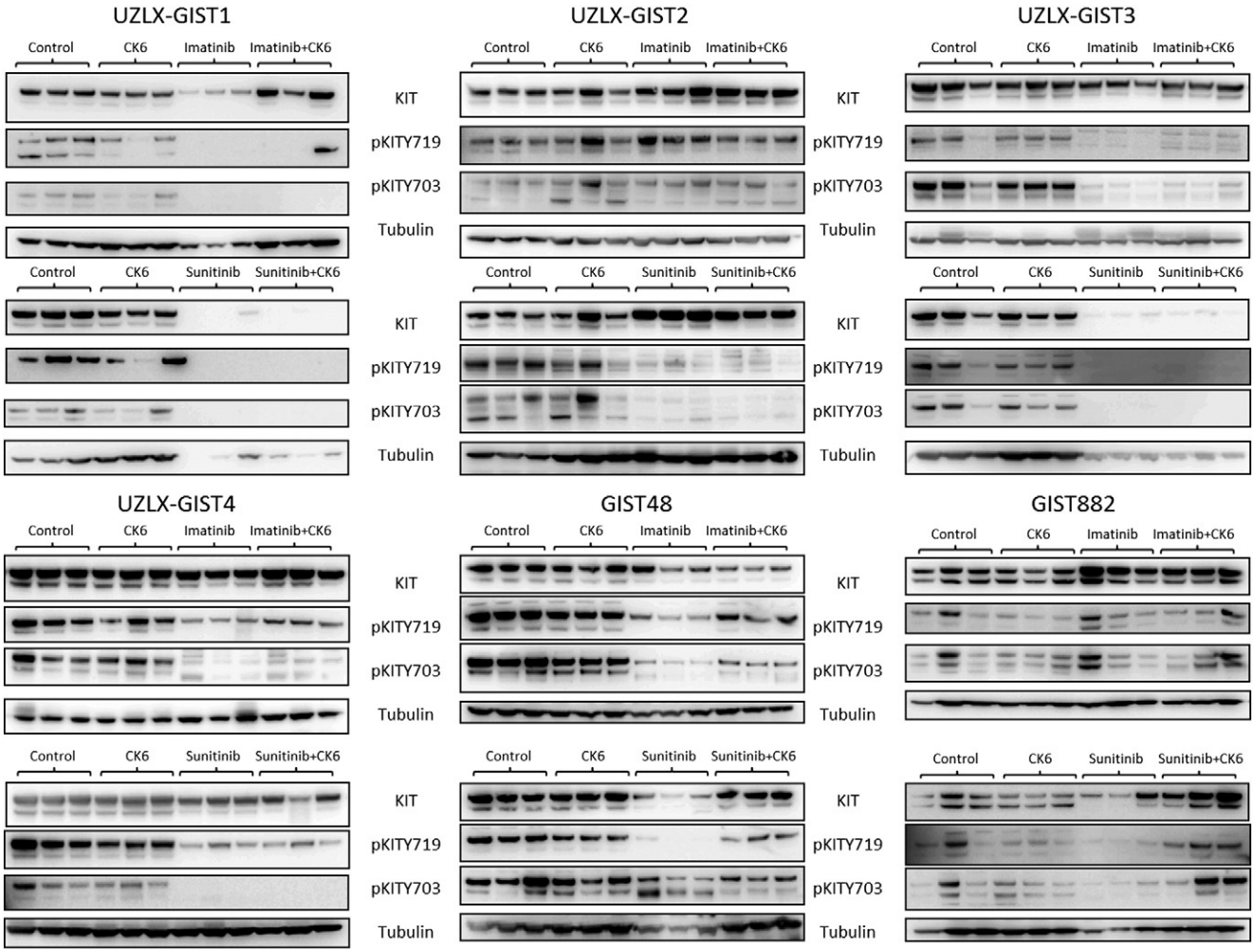

Figure 2. Western blot analysis for tumors collected after 3 weeks of treatment grouped by treatment.

induced a pronounced decrease in KIT activation in all other xenograft models tested (Figure 2).

Under CK6 alone, we did not observe an inhibition of KIT expression or activation in any of the GIST xenografts except in the UZLX-GIST1 model (Figure 2). Furthermore, we did not observe enhanced decrease in KIT activation on TKI therapy combination with CK6. Interestingly, in the GIST48 model, single TKI treatment seemed more potent in decreasing KIT phosphorylation compared to combination therapy (Figure 2).

Of note, especially in the UZLX-GIST1, UZLX-GIST3, and GIST48 models, equal protein loading was not optimal particularly in sunitinib and sunitinib + CK6 cohorts. This observation is most likely related to the extensive myxoid degeneration observed in those tumors, leaving almost no viable cells.

Discussion

Despite the remarkable clinical success of imatinib treatment in GIST, the majority of patients develop secondary resistance to this agent [7–9,12]. To date, imatinib resistant or intolerant patients are treated with sunitinib and regorafenib as a second- or third-line treatment. However, the duration of progression-free survival in the clinic declines progressively with every further line of treatment. Hence, there is an important need for alternative treatment methods beyond the traditional small molecule TKI approach in GIST. In the majority of cases, secondary resistance mutations are situated in the intracellular TK1 and TK2 domains of the KIT receptor. Therefore, targeting the EC domain with monoclonal antibodies could be a valuable treatment approach in GIST.

In the current study, we have evaluated the efficacy of CK6, a fully human anti-KIT monoclonal antibody binding to the EC region of the KIT protein, as a single agent and in combination with TKIs used as standard of care (imatinib and sunitinib) in GIST. CK6 as a single agent did not efficiently reduce tumor volume in any of the GIST xenograft models used in this study. We only observed a delay in tumor growth in UZLX-GIST3 compared to the untreated control group. CK6 did not induce a significant decrease in mitotic activity, and apoptotic activity was only slightly increased in UZLX-GIST1, UZLX-GIST4, and GIST48 (1.4- to 1.5-fold of the untreated controls), although these increases were not statistically significant. In UZLX-GIST1, CK6 showed only a minor inhibitory effect on KIT phosphorylation; this effect was not observed in other GIST xenograft models. In general, the combination of CK6 with TKIs did not lead to improved efficacy of either sunitinib or imatinib compared to the single-agent regimens in our patient-derived mouse xenograft GIST models. Recently, Edris and colleagues have shown the potential of the anti-KIT monoclonal antibody SR1 both *in vitro* and *in vivo*[13]. In their study, SR1 yielded a significantly decreased GIST tumor cell growth and cell surface KIT expression as well as increased macrophage phagocytosis. There might be several reasons for higher efficacy of SR1 in comparison to CK6. First of all, there may be different affinity of the antibodies to different mutated form of KIT receptor. In our study, we have used six different models characterized by different KIT mutations. Only one model—cell line–derived GIST882—was used in both studies and, in the experiment with SR1, produced smaller tumors than in GIST430, yet with strong *in vivo* inhibition by the antibody. Additionally, for our experiments, we used subcutaneous transplantation of tumor fragments, while in the study testing SR1, tumors were induced through i.p. injection of transduced cells. The direct and more efficient delivery of SR1 through i.p. injection and its penetration to tumors localized i.p. may explain better efficacy in the study of Edris et al. Additionally, the microenvironment in the i.p. engrafted tumors could influence the tumor cells. Finally, since at least partially the response to SR1 was assigned to the increased macrophage phagocytosis, also the usage of different strains of immunosuppressed mouse for *in vivo* experiments in both our study and that of Edris et al. cannot be excluded as the reasons for the different levels of efficiency observed in both studies.

There could be several explanations for the lack of efficacy of the CK6 antibody in our GIST xenograft models. Tabone-Eglinger and colleagues have shown that *KIT* mutations in GIST induce aberrations in the normal maturation and trafficking of the KIT protein [22]. These alterations can lead to intracellular retention of the activated RTK in the cell. This observation is also supported by Xiang et al., who have shown that intracellular KIT signaling could be sufficient to drive oncogenesis in KIT-dependent malignancies [23]. Therefore, the lack of antagonistic effects on KIT could be related to conformational changes imposed by activating *KIT* mutations, possibly mediated through maturation and trafficking of the protein that may eventually not reach the cell surface. Second, monoclonal antibodies as large molecules cannot be delivered to the cytoplasmic cell compartment. Hence, if the majority of highly active KIT oncoproteins are located intracellularly, the effect of the antibody on plasma membrane–associated KIT could be masked by a dominant intracellular KIT activation. This could explain why we see a lack of effect under CK6 treatment in the GIST xenografts tested, while CK6 showed KIT antagonist effects in melanoma, small cell lung carcinoma, and leukemia research models [14]. Therefore, we would suggest further studies characterizing the binding properties of anti-KIT monoclonal antibodies to the GIST mutant KIT receptor along with thorough analysis of KIT receptor localization in GIST models. In addition, due to intracellular retention of mutated KIT oncoproteins, methods should be explored to deliver the active agents to the intracellular compartment without interfering with the target specificity [22].

Furthermore, in our study, we had some evidence for antagonism between CK6 and TKIs in GIST models. Although this observation was not fully consistent throughout our different experiments, it warrants further exploration to better understand potential biologic mechanism of action contributing to these combination effects. A first mechanism that could explain this observation might be that the monoclonal antibody is not able to bind potently to all KIT mutants, due to possible conformational changes caused by the *KIT* mutation. Due to the heterozygous nature of *KIT* mutations in our models and in the majority of GISTs, a portion of wild-type KIT is also present. Therefore, if the antibody still binds the wild-type KIT receptor and targets it for proteasomal degradation, this will lead to a prevalence of only mutant KIT oncoproteins forming homodimers, resulting in a functional KIT homozygote. The presence of homozygous *KIT* mutations has been associated with more malignant behavior and tumor progression in GIST [24,25]. Finally, binding of the antibody could induce conformational changes depending on the *KIT* genotype, and it has been shown that sensitivity to TKIs is highly dependent on the conformation of the KIT protein [26–28]. In addition, the suggested conformational change could also lead to a facilitation of receptor dimerization, which may result in increased oncogenic signaling [29].

In conclusion, we were not able to demonstrate significant anti-tumor effects of CK6, a monoclonal KIT antibody, in our GIST

xenograft models under the applied experimental conditions. Moreover, we did not observe synergy of the agent with TKIs, but some of our findings suggest that such combination in GIST could lead to decreased anti-tumor efficacy. Our results warrant further exploration of the properties of monoclonal antibodies in relation to the different mutational variants of KIT oncoprotein *in vitro* and *in vivo*. Additional preclinical studies testing the combination of small molecule kinase inhibitors with KIT-specific antibodies should be designed in a way to specifically detect, through extensive molecular analysis, any potential antagonism between these two drug classes.

Acknowledgements

The authors thank Jesse Kimman for his excellent technical support.

References

[1] Rubin BP, Heinrich MC, and Corless CL (2007). Gastrointestinal stromal tumour. *Lancet* **369**, 1731–1741.

[2] Miettinen M and Lasota J (2006). Gastrointestinal stromal tumors: review on morphology, molecular pathology, prognosis, and differential diagnosis. *Arch Pathol Lab Med* **130**, 1466–1478.

[3] Hirota S, Isozaki K, Moriyama Y, Hashimoto K, Nishida T, Ishiguro S, Kawano K, Hanada M, Kurata A, and Takeda M, et al (1998). Gain-of-function mutations of c-kit in human gastrointestinal stromal tumors. *Science* **279**, 577–580.

[4] Heinrich MC, Corless CL, Demetri GD, Blanke CD, von Mehren M, Joensuu H, McGreevey LS, Chen CJ, Van den Abbeele AD, and Druker BJ, et al (2003). Kinase mutations and imatinib response in patients with metastatic gastrointestinal stromal tumor. *J Clin Oncol* **21**, 4342–4349.

[5] Corless CL, Schroeder A, Griffith D, Town A, McGreevey L, Harrell P, Shiraga S, Bainbridge T, Morich J, and Heinrich MC (2005). PDGFRA mutations in gastrointestinal stromal tumors: frequency, spectrum and in vitro sensitivity to imatinib. *J Clin Oncol* **23**, 5357–5364.

[6] Debiec-Rychter M, Sciot R, Le Cesne A, Schlemmer M, Hohenberger P, van Oosterom AT, Blay JY, Leyvraz S, Stul M, and Casali PG, et al (2006). KIT mutations and dose selection for imatinib in patients with advanced gastrointestinal stromal tumours. *Eur J Cancer* **42**, 1093–1103.

[7] Debiec-Rychter M, Cools J, Dumez H, Sciot R, Stul M, Mentens N, Vranckx H, Wasag B, Prenen H, and Roesel J, et al (2005). Mechanisms of resistance to imatinib mesylate in gastrointestinal stromal tumors and activity of the PKC412 inhibitor against imatinib-resistant mutants. *Gastroenterology* **128**, 270–279.

[8] Gramza AW, Corless CL, and Heinrich MC (2009). Resistance to tyrosine kinase inhibitors in gastrointestinal stromal tumors. *Clin Cancer Res* **15**, 7510–7518.

[9] Liegl B, Kepten I, Le C, Zhu M, Demetri GD, Heinrich MC, Fletcher CD, Corless CL, and Fletcher JA, et al (2008). Heterogeneity of kinase inhibitor resistance mechanisms in GIST. *J Pathol* **216**, 64–74.

[10] Demetri GD, van Oosterom AT, Garrett CR, Blackstein ME, Shah MH, Verweij J, McArthur G, Judson IR, Heinrich MC, and Morgan JA, et al (2006). Efficacy and safety of sunitinib in patients with advanced gastrointestinal stromal tumour after failure of imatinib: a randomised controlled trial. *Lancet* **368**, 1329–1338.

[11] Demetri GD, Reichardt P, Kang YK, Blay JY, Rutkowski P, Gelderblom H, Hohenberger P, Leahy M, von Mehren M, and Joensuu H, et al (2013). Efficacy and safety of regorafenib for advanced gastrointestinal stromal tumours after failure of imatinib and sunitinib (GRID): an international, multicentre, randomised, placebo-controlled, phase 3 trial. *Lancet* **381**(9863), 295–302.

[12] Corless CL, Barnett CM, and Heinrich MC (2011). Gastrointestinal stromal tumours: origin and molecular oncology. *Nat Rev Cancer* **11**, 865–878.

[13] Edris B, Willingham SB, Weiskopf K, Volkmer AK, Volkmer JP, Mühlenberg T, Montgomery KD, Contreras-Trujillo H, Czechowicz A, and Fletcher JA, et al (2013). Anti-KIT monoclonal antibody inhibits imatinib-resistant gastrointestinal stromal tumor growth. *Proc Natl Acad Sci U S A* **110**, 3501–3506.

[14] Lebron MB, Brennan L, Damoci CB, Prewett MC, O'Mahony M, Duignan IJ, Credille KM, DeLigio JT, Starodubtseva M, and Amatulli M, et al (2014). A human monoclonal antibody targeting the stem cell factor receptor (c-Kit) blocks tumor cell signaling and inhibits tumor growth. *Cancer Biol Ther* **15**, 1208–1218.

[15] Floris G, Debiec-Rychter M, Sciot R, Stefan C, Fieuws S, Machiels K, Atadja P, Wozniak A, Faa G, and Schöffski P (2009). High efficacy of panobinostat towards human gastrointestinal stromal tumors in a xenograft mouse model. *Clin Cancer Res* **15**, 4066–4076.

[16] Floris G, Sciot R, Wozniak A, Van Looy T, Wellens J, Faa G, Normant E, Debiec-Rychter M, and Schöffski P (2011). The novel HSP90 inhibitor, IPI-493, is highly effective in human gastrostrointestinal stromal tumor xenografts carrying heterogeneous *KIT* mutations. *Clin Cancer Res* **17**, 5604–5614.

[17] Floris G, Debiec-Rychter M, Wozniak A, Stefan C, Normant E, Faa G, Machiels K, Vanleeuw U, Sciot R, and Schöffski P (2011). The heat shock protein 90 inhibitor IPI-504 induces KIT degradation, tumor shrinkage, and cell proliferation arrest in xenograft models of gastrointestinal stromal tumors. *Mol Cancer Ther* **10**, 1897–1908.

[18] Floris G, Wozniak A, Sciot R, Li H, Friedman L, Van Looy T, Wellens J, Vermaelen P, Deroose CM, and Fletcher JA, et al (2013). A potent combination of the novel PI3K Inhibitor, GDC-0941, with imatinib in gastrointestinal stromal tumor xenografts: long-lasting responses after treatment withdrawal. *Clin Cancer Res* **19**, 620–630.

[19] Antonescu CR, Besmer P, Guo T, Arkun K, Hom G, Koryotowski B, Leversha MA, Jeffrey PD, Desantis D, and Singer S, et al (2005). Acquired resistance to imatinib in gastrointestinal stromal tumor occurs through secondary gene mutation. *Clin Cancer Res* **11**, 4182–4190.

[20] Agaram NP, Besmer P, Wong GC, Guo T, Socci ND, Maki RG, DeSantis D, Brennan MF, Singer S, and DeMatteo RP, et al (2007). Pathologic and molecular heterogeneity in imatinib-stable or imatinib-responsive gastrointestinal stromal tumors. *Clin Cancer Res* **13**, 170–181.

[21] Rossi F, Ehlers I, Agosti V, Socci ND, Viale A, Sommer G, Yozgat Y, Manova K, Antonescu CR, and Besmer P (2006). Oncogenic Kit signaling and therapeutic intervention in a mouse model of gastrointestinal stromal tumor. *Proc Natl Acad Sci U S A* **103**, 12843–12848.

[22] Tabone-Eglinger S, Subra F, El Sayadi H, Alberti L, Tabone E, Michot JP, Théou-Anton N, Lemoine A, Blay JY, and Emile JF (2008). KIT mutations induce intracellular retention and activation of an immature form of the KIT protein in gastrointestinal stromal tumors. *Clin Cancer Res* **14**, 2285–2294.

[23] Xiang Z, Kreisel F, Cain J, Colson A, and Tomasson MH (2007). Neoplasia driven by mutant c-KIT is mediated by intracellular, not plasma membrane, receptor signaling. *Mol Cell Biol* **27**, 267–282.

[24] Chen LL, Holden JA, Choi H, Zhu J, Wu EF, Jones KA, Ward JH, Andtbacka RH, Randall RL, and Scaife CL, et al (2008). Evolution from heterozygous to homozygous KIT mutation in gastrointestinal stromal tumor correlates with the mechanism of mitotic nondisjunction and significant tumor progression. *Mod Pathol* **21**, 826–836.

[25] Lasota J, vel Dobosz AJ, Wasag B, Wozniak A, Kraszewska E, Michej W, Ptaszynski K, Rutkowski P, Sarlomo-Rikala M, and Steigen SE, et al (2007). Presence of homozygous KIT exon 11 mutations is strongly associated with malignant clinical behavior in gastrointestinal stromal tumors. *Lab Invest* **87**, 1029–1041.

[26] Mol CD, Lim KB, Sridhar V, Zou H, Chien EY, Sang BC, Nowakowski J, Kassel DB, Cronin CN, and McRee DE (2003). Structure of a c-kit product complex reveals the basis for kinase transactivation. *J Biol Chem* **278**, 31461–31464.

[27] Mol CD, Dougan DR, Schneider TR, Skene RJ, Kraus ML, Scheibe DN, Snell GP, Zou H, Sang BC, and Wilson KP (2004). Structural basis for the autoinhibition and STI-571 inhibition of c-Kit tyrosine kinase. *J Biol Chem* **279**, 31655–31663.

[28] Gajiwala KS, Wu JC, Christensen J, Deshmukh GD, Diehl W, DiNitto JP, English JM, Greig MJ, He YA, and Jacques SL, et al (2009). KIT kinase mutants show unique mechanisms of drug resistance to imatinib and sunitinib in gastrointestinal stromal tumor patients. *Proc Natl Acad Sci U S A* **106**, 1542–1547.

[29] Kurosawa K, Miyazawa K, Gotoh A, Katagiri T, Nishimaki J, Ashman LK, and Toyama K (1996). Immobilized anti-KIT monoclonal antibody induces ligand-independent dimerization and activation of Steel factor receptor: biologic similarity with membrane-bound form of Steel factor rather than its soluble form. *Blood* **87**, 2235–2243.

[30] Bauer S, Duensing A, Demetri GD, and Fletcher JA (2007). KIT oncogenic signalling mechanisms in imatinib-resistant gastrointestinal stromal tumor: PI3-kinase/AKT is a crucial survival pathway. *Oncogene* **26**, 7560–7568.